

TRANSVERSE-TRANSVERSE AND TRANSVERSE-LONGITUDINAL PHASE-SPACE CONVERTERS FOR ENHANCED BEAM APPLICATIONS

K.-J. Kim, ANL, Argonne, IL 60439, U.S.A.

Abstract

Emittance exchange and flat beam transform are two phase-space converting techniques being developed recently to enhance the performance of electron beams for various applications. We review these applications, the basic principles of the converters, and the status of experimental demonstration of these techniques.

EMITTANCE EXCHANGE AND FLAT BEAM TRANSFORM

The emittance exchange (EEX) is an interchange of the distributions in two separate 2-D subspaces of the 6-D phase space [1,2]. Figure 1 illustrates the exchange between the transverse (x, x') space and the longitudinal (z, δ) space. In this exchange, the emittances in the x - and the z -directions, ϵ_x and ϵ_z , become interchanged into ϵ_z and ϵ_x . Although the exchange is feasible between any two subspaces, we limit the discussion in this paper to the exchange between the (x, x') and (z, δ) subspaces.

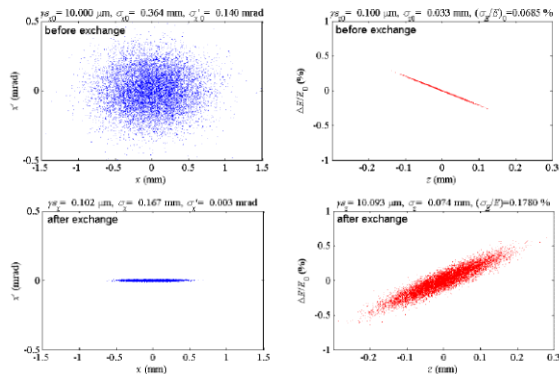


Figure 1: Emittance exchange: The top and bottom graphs are the distributions before and after the EEX, respectively, while the left (blue) and right (red) graphs are the distributions in the transverse and longitudinal phase space, respectively (courtesy of P. Emma).

The flat beam transform (FBT) is a technique to change a round beam from a source with equal x - and y -emittances $\epsilon_x^0 = \epsilon_y^0$ to a flat beam with unequal emittances ϵ_x and ϵ_z of an arbitrary ratio ϵ_x/ϵ_z , keeping the product fixed; $\epsilon_x^0 \epsilon_y^0 = \epsilon_x \epsilon_y$ [3,4].

These phase-space-converting techniques, individually or in combination, can enhance the power of particle beams for certain applications, as discussed in the following section.

*Work supported by U.S. Department of Energy, Office of Science, Office of Basic Energy Sciences, under Contract No. DE-AC02-06CH11357.

APPLICATIONS

We discuss some examples of application of the phase-space-converting techniques in high-gain free-electron lasers (FELs), linear colliders, high-power infrared (IR) FELs, and Smith-Purcell backward-wave oscillators (BWOs).

Matched Beams for High-Gain FELs

For optimum performance of a free-electron laser (FEL), the emittance of the driving electron beam should not be larger than that of the radiation beam:

$$\epsilon_x \leq \gamma \lambda / 4\pi, \quad (1)$$

where λ and γ are the radiation wavelength and electron energy in units of its rest energy, respectively. Throughout this paper, emittances will be understood to be the rms, normalized value. For a 1-Å FEL driven by 5-GeV electron beams, the matched emittance is then $\epsilon_x \sim 0.1 \mu\text{m}$, an order of magnitude smaller than achievable by the current state-of-the-art injectors. In the current high-gain x-ray FEL projects, such as the Linac Coherent Light Source (LCLS) [5] and the European x-FEL [6], the reduction in gain arising from the violation of the matching condition is partially overcome by increasing the current and the energy of the electron beam to a few kA and to $E > 15$ GeV, respectively. The deflection parameter needs to be also increased, to $K \sim 3.7$ for the LCLS.

Electron beams matched to high-gain x-FEL operation can be produced by a combined use of EEX and FBT as follows [2]. The measured slice energy spread from a photocathode gun for 4-nC beam is about 4 keV [7]. For the low-charge case (30 pC) considered here, we may assume that the rms energy spread is $\sigma_{\Delta E} = 1.5$ keV, corresponding to the rms spread of γ , $\sigma_{\Delta \gamma} = 0.003$. The longitudinal emittance of a short electron beam of rms length $\sigma_z = 34 \mu\text{m}$ then becomes $\epsilon_z = \sigma_z \sigma_{\Delta \gamma} = 0.1 \mu\text{m}$. Assuming that the gun current is $I = 100\text{A}$, the bunch charge is 28 pC. In the transverse dimensions, a round beam with $\epsilon_x^0 = \epsilon_y^0 = 1 \mu\text{m}$ is transformed via FBT to obtain a flat beam with $(\epsilon_x, \epsilon_y) = (10, 0.1) \mu\text{m}$. The x - and the z -emittances are then exchanged, giving rise to the final partition of emittances $(\epsilon_x, \epsilon_y, \epsilon_z) = (0.1, 0.1, 10) \mu\text{m}$. The transverse emittances are now matched to the x-ray emittance. The longitudinal phase space should then be adjusted at some convenient point before the FEL so that the relative energy spread becomes smaller than the maximum allowed for the FEL operation, about 10^{-4} . The bunch length then becomes $3.4 \mu\text{m}$ at 15 GeV, about ten times shorter. The current therefore becomes about ten

times higher, $I = 1$ kA. Figure 2 shows the advantages of the matched electron beam for a future “green field,” 0.4-Å FEL [8] by plotting the gain length as a function of K , assuming that the undulator period is 3 cm and the relative energy spread is 10^{-4} . (The electron energy is determined from the resonance condition.) Curve (a) corresponds to the case of the LCLS with $I = 3.5$ kA and $\varepsilon_x = \varepsilon_y = 1$ μm , while curve (b) corresponds to the matched case with $I = 1$ kA and $\varepsilon_x = \varepsilon_y = 0.1$ μm . The gain length for curve (b) is shorter by more than a factor of three than that of curve (a). In addition, the gain is almost independent of the K for curve (b), permitting the use of a small value of K . A smaller value of K has advantages since the resonant electron energy is lower, making the device less expensive and also suppressing the harmful spontaneous radiation at high harmonics.

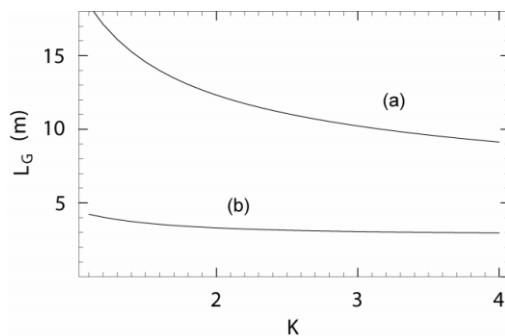


Figure 2: Comparison of FEL performances (courtesy of Z. Huang).

ILC Electron Beams without Damping Ring

The transverse emittances of the electron and positron beams in a linear collider should be small for high-luminosity operation. The emittance in the vertical (y) direction needs to be particularly small to suppress quantum bremsstrahlung. The emittances in the current International Linear Collider (ILC) design are $(\varepsilon_x, \varepsilon_y, \varepsilon_z) = (8, 0.02, 3000)$ μm for each 3-nC bunch [9]. These bunches are to be produced from two 5-GeV, 6-km damping rings, one for electrons and one for positrons.

For the electrons, beams of similar characteristics can be produced in a compact system consisting of an rf photocathode gun and phase-space converters. Since the geometric average of the required transverse emittances, $\varepsilon_T = \sqrt{\varepsilon_x \varepsilon_y} = 0.4$ μm , is not very small, a future rf photocathode gun may be able to produce a round, 3-nC bunches with the transverse emittance ε_T . In that case, the ILC electron beam can be produced by an FBT technique alone. Otherwise we can start from $(\varepsilon_x, \varepsilon_y, \varepsilon_z) = (1, 1, 8)$ μm , perform an FBT to obtain $(50, 0.02, 8)$ μm , and finally obtain $(8, 0.02, 50)$ μm by an (x - z) EEX. Note that the longitudinal emittance in the final emittance partition is much smaller than the ILC specification.

EEX for MW-Class IR FEL

A major problem for designing a MW-class IR FEL based on an energy recovery linac (ERL) for industrial/military application is how to dispose of the high-power electron beam with a negligible loss. This is a serious issue since the energy spread induced by the FEL interaction becomes a large relative spread when the electrons are decelerated to a low energy before the dump. The usual approach is to rely on beam manipulation in longitudinal phase space—rotating the beam in the longitudinal phase space to reduce the energy spread before deceleration [10].

The emittance exchange may provide a more versatile solution than one based on longitudinal manipulation alone. A preliminary concept by P. Piot is illustrated in Fig. 3, where the transverse and longitudinal beam phase-space distributions at different points are schematically illustrated by red and green ellipses, respectively. An EEX section is inserted between the FEL exit and the return arc. Before the EEX, the transverse beam parameters are matched such that they provide the desired bunch length and correlated energy spread after the EEX and before deceleration starts.

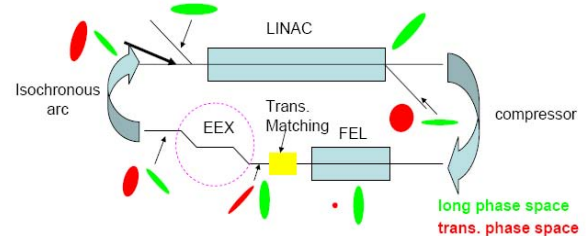


Figure 3: An ERL/FEL configuration with an EEX section to minimize the beam loss (courtesy of P. Piot).

Smith-Purcell BWO for Terahertz Radiation

A Smith-Purcell BWO is interesting as a potential source of intense Terahertz radiation [11-14]. For a tight beam-grating coupling, electrons must travel close to the grating surface at a distance Δy . For a grating length L , the restriction to the emittance in the direction normal to the grating surface, the y -direction, is $\varepsilon_y \leq \beta\gamma(\Delta y)^2 / L$.

In the case studied in Ref. 14, $\beta\gamma = 0.35$, $L = 2$ cm, and $\Delta y = 20$ mm, thus $\varepsilon_y < 3 \cdot 10^{-3}$ μm . The FBT technique is well suited for producing such a beam.

PRINCIPLES

We will now summarize basic principles of phase-space converters.

Emittance Exchange Theorem

The particle coordinates in the (x - z) phase space is defined by either the column vector X or row vector \tilde{X} , where the tilde denotes the transpose operation:

$$X = \begin{pmatrix} x \\ x' \\ z \\ \delta \end{pmatrix}, \tilde{X} = (x, x', z, \delta) \quad (2)$$

The beam matrix is defined by

$$\Sigma = \langle X \tilde{X} \rangle = \begin{bmatrix} \langle x^2 \rangle & \langle xx' \rangle & \langle xz \rangle & \langle x\delta \rangle \\ \langle xx' \rangle & \cdot & \cdot & \cdot \\ \langle xz \rangle & \cdot & \cdot & \cdot \\ \langle x\delta \rangle & \cdot & \cdot & \langle \delta^2 \rangle \end{bmatrix}, \quad (3)$$

where the angular brackets denote taking the average. The beam matrix is decomposed into 2×2 submatrices as follows:

$$\Sigma = \begin{bmatrix} \Sigma_x & \Sigma_c \\ \tilde{\Sigma}_c & \Sigma_z \end{bmatrix}. \quad (4)$$

The emittances are defined as

$$\varepsilon_x = \sqrt{\text{Det}(\Sigma_x)}, \varepsilon_z = \sqrt{\text{Det}(\Sigma_z)}. \quad (5)$$

These are referred to as the ‘‘projected’’ emittances if the coupling $\text{Det}(\Sigma_c)$ does not vanish. The emittance concept is most useful when the beam matrix is ‘‘uncoupled,’’ that is, when $\text{Det}(\Sigma_c) = 0$.

Consider a beamline giving rise to a linear transformation of the phase-space vector

$$X \rightarrow MX. \quad (6)$$

For a Hamiltonian system, the transformation matrix M is symplectic:

$$\tilde{M}JM = J, \quad (7)$$

where J is the unit symplectic matrix:

$$J = \begin{bmatrix} J_{2D} & 0 \\ 0 & J_{2D} \end{bmatrix}, J_{2D} = \begin{bmatrix} 0 & 1 \\ -1 & 0 \end{bmatrix}. \quad (8)$$

Equation (7) implies that the following two quantities are conserved under the transformation M :

$$\varepsilon_{4d} = \text{Det}(\Sigma) \quad \text{and} \quad I^{(2)} = -\frac{1}{2} T_r(\Sigma J \Sigma). \quad (9)$$

Suppose M connects an uncoupled beam matrix to another uncoupled one. From the existence of two invariants, one can show that the emittances transform in either of the following two ways:

$$(\varepsilon_x, \varepsilon_y) \rightarrow (\varepsilon_x, \varepsilon_y), \quad (10)$$

or

$$(\varepsilon_x, \varepsilon_z) \rightarrow (\varepsilon_z, \varepsilon_x). \quad (11)$$

In the first case, the emittances are separately conserved, while they are completely exchanged in the second case, Eq. (11). This is the emittance exchange theorem first proved by E. Courant [15].

Construction of Exact (x, z) Exchange

An exact exchange is a transformation for which the two off-diagonal 2×2 submatrices of the transformation matrix M vanish. A necessary condition for such a transformation is that it cancels out an arbitrary initial energy deviation δ for a particle with initial $x = x' = 0$. Consider a dispersive element producing a dispersion η followed by a deflection cavity producing an x -dependent δ -kick of coefficient k . The energy of the particle after the dog-leg and the transverse cavity is $\delta + k \times (\eta\delta)$, which vanishes if $k = -1/\eta$.

A beamline in which a transverse cavity is sandwiched by two identical dog-legs, as sketched in Fig. 4, was shown by the author to induce an exact $(x-z)$ exchange [16]. This is a refinement of an earlier, approximate exchange scheme in which the second dogleg is in the reverse direction [1]. The fact that the beamline shown in Fig. 4 produces an exact exchange can be verified by using the following expressions for the matrices of a dogleg and a thin cavity ($k = -1/\eta$):

$$M_{\text{dogleg}} = \begin{bmatrix} 1 & L & 0 & \eta \\ 0 & 1 & 0 & 0 \\ 0 & \eta & 1 & \xi \\ 0 & 0 & 0 & 1 \end{bmatrix}, M_{\text{cav}} = \begin{bmatrix} 1 & 0 & 0 & 0 \\ 0 & 1 & k & 0 \\ 0 & 0 & 1 & 0 \\ k & 0 & 0 & 1 \end{bmatrix}. \quad (12)$$

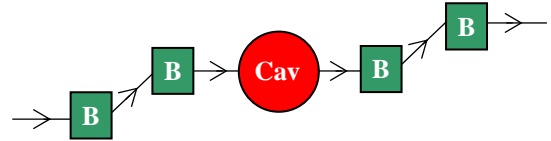


Figure 4: An exact exchange beamline.

A more general method for finding exact exchange was discussed by R. Fliller [17] based on the configuration shown in Fig. 5.

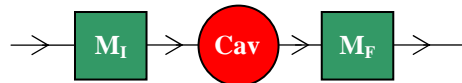


Figure 5: A general structure for exact emittance exchange.

Here, the cavity matrix is taken to be given by Eq. (12), and the matrices for the static elements M_I and M_F are in the following form constrained by the symplecticity:

$$M_I = \begin{bmatrix} a & b & 0 & \eta \\ c & d & 0 & \eta' \\ a\eta - b\eta' & c\eta - d\eta' & 1 & \xi \\ 0 & 0 & 0 & 1 \end{bmatrix}, \quad (14)$$

$$M_F = \begin{bmatrix} e & f & 0 & D \\ g & h & 0 & D' \\ gD - eD' & hD - fD' & 1 & \chi \\ 0 & 0 & 0 & 1 \end{bmatrix}.$$

The condition $k = -1/\eta$ is still imposed. We then find that the condition that the total matrix $M = M_F M_{CAV} M_I$ becomes an exact exchange is

$$\begin{pmatrix} e & f \\ g & h \end{pmatrix} \begin{pmatrix} \eta \\ \eta' \end{pmatrix} = \begin{pmatrix} D \\ D' \end{pmatrix}. \quad (15)$$

A simple solution Eq. (15) is to choose $\eta = 0$ and $M_I = M_I = M_{dogleg}$, shown in Fig. 4 [16]. Recently, H. Edwards found another solution in which M_F consists of a quadrupole magnet followed by a dipole [18].

Flat-Beam Generation

The principles of FBT are illustrated by Fig. 6:

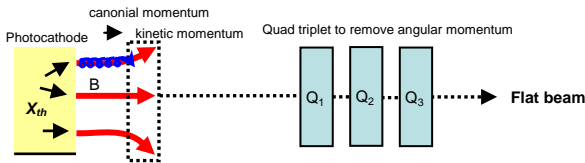


Figure 6: A schematic of FBT.

Electrons are produced with canonical angular momentum from a photocathode immersed in an axial magnetic field B . The canonical angular momentum is converted into kinetic angular momentum as the beam leaves the magnetic field region. A set of quadrupoles then removes the kinetic angular momentum and the beam becomes flat as a consequence [19]. The process can be analyzed by different methods [20,21]. Below we follow the analysis of Ref. 21.

The motion of an electron in an axial magnetic field is conveniently studied in a frame rotating around the z -axis with the spatial angular frequency $\kappa = qB/2mc$, since the transverse motion in this frame is a simple betatron motion of variable focusing strength [22]

$$(x, y)'' + \kappa^2(x, y) = 0. \quad (16)$$

Let the transverse phase space coordinates of an electron as it leaves the cathode surface be $\tilde{X}_{th} = (x, x', y, y')$. The corresponding beam matrix averaged over the electrons' thermal motion is

$$\Sigma_{th} = \langle X_{th} \tilde{X}_{th} \rangle = \begin{bmatrix} \varepsilon_{th} T_{th} & 0 \\ 0 & \varepsilon_{th} T_{th} \end{bmatrix}, \quad (17)$$

where

$$\varepsilon_{th} = \sigma_x \sigma_{x'}, T_{th} = \begin{bmatrix} \beta_{th} & 0 \\ 0 & 1/\beta_{th} \end{bmatrix}, \beta_{th} = \frac{\sigma_x}{\sigma_{x'}}.$$

Here $\sigma_x = \sqrt{\langle x^2 \rangle}$ and $\sigma_{x'} = \langle x'^2 \rangle$. Since the motion is viewed in a rotating frame in the presence of a magnetic field, the electron's phase-space coordinates become $\tilde{X}_0 = (x, x' - \kappa y, y, y' + \kappa x)$. The beam matrix is then in the form

$$\Sigma_0 = \langle X_0 \tilde{X}_0 \rangle = \begin{bmatrix} \varepsilon_{eff} T_0 & \mathcal{L} J \\ -\mathcal{L} J & \varepsilon_{eff} T_0 \end{bmatrix}, \quad (18)$$

where

$$\varepsilon_{eff} = \sqrt{\varepsilon_{th}^2 + \mathcal{L}^2}, T_0 = \begin{bmatrix} \beta_0 & 0 \\ 0 & 1/\beta_0 \end{bmatrix}, \mathcal{L} = \kappa \sigma_x^2. \quad (19)$$

The action of the quadrupoles removing the angular momentum can be represented by a symplectic matrix M_Q :

$$M_Q \Sigma \tilde{M}_Q = \begin{bmatrix} \varepsilon_+ T_+ & 0 \\ 0 & \varepsilon_- T_- \end{bmatrix}, T_{\pm} = \begin{bmatrix} 1/\beta_{\pm} & 0 \\ 0 & 1/\beta_{\pm} \end{bmatrix}. \quad (20)$$

Since M_Q is symplectic, the quantities I_2 and ε_{AD} introduced in Eq. (9) are both conserved. It then follows that

$$\varepsilon_{\pm} = \varepsilon_{eff} \pm \mathcal{L}, \quad \varepsilon_{th} = \sqrt{\varepsilon_+ \varepsilon_-}. \quad (21)$$

When $\mathcal{L} \gg \varepsilon_{th}$, as is usually the case, the beam becomes very flat with the emittance ratio

$$\frac{\varepsilon_+}{\varepsilon_-} \approx \left(\frac{2\mathcal{L}}{\varepsilon_{th}} \right)^2. \quad (22)$$

Note that the emittance ratio may be adjusted arbitrarily in FBT by adjusting the magnetic field. This is in contrast to the case of EEX where the final emittances are fixed by the initial values. Does FBT then violate the emittance exchange theorem? It does not, since the transformation $X_{th} \rightarrow X_0$ is non-symplectic. We can also say that the theorem is not violated since the coupling does not vanish in the beam matrix Σ_0 ; in fact, the coupling is the angular momentum.

DEMONSTRATION EXPERIMENTS

Flat-Beam Production

A demonstration experiment for FBT was performed at the Fermilab A0 facility led by D. Edwards and H. Edwards, achieving an emittance ratio of 40 [23]. A study of the effects limiting the ratio was performed by Y.-e. Sun as a part of her thesis research at the University of Chicago [24]. The ratio was later increased to 100 by P. Piot et al. [25]. Further work is necessary since the emittance ratio required for applications is about 1000.

Emittance Exchange Experiment

Demonstration experiments for EEX are being pursued at two facilities, the Fermilab A0 and Argonne AWA. The status of the Fermilab experiment is reported in these proceedings [26]. The beamline is in a double dogleg configuration as in Fig. 4. A 5-cell, 3.9-GHz deflecting cavity is fabricated for operation at LiN temperature [27]. The plan for the first experiment is to perform EEX $(\epsilon_x, \epsilon_y, \epsilon_z) = (4,4,130) \mu\text{m} \rightarrow (130,3,3) \mu\text{m}$.

The Argonne AWA experiment is being pursued as a collaboration of ANL-APS, ANL-HEP, NIU, and Tsinghua University [28]. The beamline will again be in a double dogleg configuration. A (1/2)-1-(1/2) cell, L-band deflecting cavity is under construction at Tsinghua University. The initial emittances in this experiment planned at this time are $(\epsilon_x, \epsilon_y, \epsilon_z) = (9,9,4) \mu\text{m}$, which will become (4,9,4) μm after EEX. The small longitudinal emittance will be generated by employing a short laser pulse, 600 fs. The emittance evolution from the cathode to the beginning of the exchanger is shown in Fig. 7.

Demonstration experiments must deal with various effects not described by theoretical discussions in terms of ideal elements, such as the finite length of the cavity, nonlinearities, etc. [29,30]. Care must also be exercised in properly assessing instabilities such as those due to CSR. A suite of diagnostics that can satisfactorily measure the relevant elements of the beam matrix will be essential for the success of these experiments. This is a challenging but worthwhile effort in view of the promising applications of the phase-space converters.

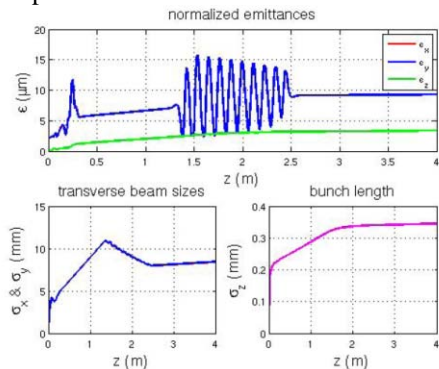


Figure 7: Emittance evaluation from the cathode to the exchanger for the ANL experiment (courtesy of M. Rihai).

ACKNOWLEDGEMENTS

The author thanks, without explicitly naming them, his colleagues at Argonne, Fermilab, NIU, SLAC, and Tsinghua University for discussions, inspirations, and suggestions on beam physics of phase-space converters.

REFERENCES

[1] M. Cornacchia and P. Emma, Phys. Rev. ST AB 5, 084001 (2002).

[2] P. Emma et al., Phys. Rev. ST AB 9, 100702, (2006).
 [3] Ya. Derbenev, University of Michigan Report No. UM-HE-98-04, 1998.
 [4] R. Brinkmann, Y. Derbenev, and K. Flöttmann, DESY Report No. TESLA 99-09, 1999; Phys. Rev. ST AB 4, 053501 (2001).
 [5] Linac Coherent Light Source Conceptual Design Report, SLAC-R-593, 2002.
 [6] TESLA XFEL Technical Design Report Supplement, TESLA FEL 2002-09, 2002.
 [7] K.-J. Kim, J. Galayda, and J. Murphy, presentation at BESAC Subcommittee on BES 20-Year Facility Road Map, Washington, D.C., 2003.
 [8] M. Hüning and H. Schlarb, Proc. PAC2003, Portland, OR, pp. 2074-2076, <http://www.jacow.org>.
 [9] ILC reference design report, http://media.linearcollider.org/rdr_draft_v1.pdf
 [10] P. Piot et al., Phys. Rev. ST AB, 6, 030702 (2003).
 [11] H.L. Andrews and C.A. Brau, Phys. Rev. ST AB 7, 070701 (2004).
 [12] H. L. Andrews et al., Phys. Rev. ST AB 8, 050703 (2005).
 [13] V. Kumar and K.-J. Kim, Phys. Rev. E 73, 026501 (2006).
 [14] K.-J. Kim and V. Kumar, ANL-AAI-Pub-2007-01, submitted to PRSTAB.
 [15] E. Courant in *Perspectives in Modern Physics, Essays in honor of H .A. Bethe*, R.E. Marshak, ed., Interscience Publishers (1966).
 [16] K.-J. Kim and A. Sessler, Proc. International Workshop on Beam Cooling and Related Topics, Galena, IL, AIP Conf. Proc. No. 821 (AIP, New York, 2006).
 [17] R. Fliller, Fermilab Report, Beams-doc-2553-V1 (2006).
 [18] H. Edward, private communication.
 [19] A. Burov and V. Danilov, Report No. FERMILAB-TM-2043, 1998.
 [20] A. Burov et al., Phys. Rev. E 66, 016503 (2002).
 [21] K.-J. Kim, Phys. Rev. ST AB 6, 104002 (2003).
 [22] K.-J. Kim and C-x. Wang, Phys. Rev. Lett., 85, 760 (2000).
 [23] D. Edwards et al., Proc. LINAC2000, 122 (2000) ; D. Edwards et al., Proc. PAC2001, 73 (2001).
 [24] Yin-e. Sun, U of C Thesis (2005); Yin-e. Sun et al., Proc. LINAC2004, 150 (2004),
 [25] P. Piot et al., Phys. Rev. ST AB 9, 031001, 2006.
 [26] R.P. Fliller et al., "Transverse to Longitudinal Emittance Exchange Beamline at the A0 Photoinjector," these proceedings.
 [27] T. Koeth et al., "A TM110 Cavity for Longitudinal to Transverse Emittance Exchange," these proceedings.
 [28] Y. Sun et al., "Design Study of a Transverse-to-Longitudinal EEX POP Experiment," these proceedings
 [29] J. Power, private communication.
 [30] D. Edwards, private communication.